# Application of Advanced Millimeter/ Far-Infrared Sources to Collective Thomson Scattering Plasma Diagnostics

*P. Woskobiniki, D.R. Chon, and R. J. Temkin*

Plasma Fusion Center
Massachusetts Institute of Technology,
Cambridge, MA 02139

# APPLICATION OF ADVANCED MILLIMETER/ FAR-INFRARED SOURCES TO COLLECTIVE THOMSON SCATTERING PLASMA DIAGNOSTICS

## P. Woskoboinikow, D. R. Cohn, and R. J. Temkin

*Plasma Fusion Center*
*Massachusetts Institute of Technology*
*Cambridge, MA 02139*

The application of advanced millimeter/far infrared sources to substantially improve the effectiveness of collective Thomson scattering plasma diagnostics is discussed. Gyrotrons, $CO_2$ lasers and far infrared lasers which are optically pumped with $CO_2$ laser radiation can now provide important new capabilities in terms of combined high peak power and high average power, fine frequency tunability and a wide range of operating frequencies. Their capabilities can improve the signal to noise ratio and make possible time dependent scattering measurements. Both thermal level scattering used for determination of ion temperature and low level non-thermal measurements used for the investigation of plasma turbulence and wave phenomena are considered. Rapidly pulsed gyrotrons, $CO_2$, and optically pumped lasers can provide a range of combinations of high peak power and high energy during a given time interval. The use of this high peak power – high energy tradeoff capability to maximize signal to noise ratios is discussed. Dramatic reduction in stray light, using fine frequency source tunability and gas absorption cell technology, is also discussed.

## Introduction

Collective Thomson scattering is an important diagnostic technique for the measurement of spacially localized ion temperature [1-5] and Z effective [6,7]. Also, increasing use is being made of collective Thomson scattering to study non-thermal turbulence [8-14] and plasma waves [15-18]. Application of this diagnostic technique to magnetically confined fusion plasmas requires sources in the millimeter/far-infrared (MM/FIR) range of wavelengths, defined here as the range 10 mm - 10μm. Sources in this range of wavelengths are required in order to meet conditions for collective scattering at angles sufficient for spatial resolution. In this paper we present a study of optimizing collective Thomson scattering signal to noise ratio from the point of view of MM/FIR source requirements.

Significant advances have been made recently in the technologies of high peak power MM/FIR sources. These technologies include: single mode, find frequency tunable $CO_2$ lasers [19,20]; rapidly pulsed $CO_2$ and optically pumped lasers; gyrotrons [21-23]; and optically pumped molecular Raman lasers which are continuously tuable over large fractions of the MM/FIR wavelength range [24,25]. Some of these source technologies provide an important new capability of continuous wave (cw) or quasi-cw high power operation. This capability can be used to make significant improvements in scattered signal to noise ratio as well as allow for time dependent measurements. Another capability these combined source technologies provide is flexibility in the choice of operating wavelength. This makes it possible to choose a source wavelength and technology that is optimum for a given set of plasma parameters instead of vice-versa.

Once the scattering wavelength is chosen, fine frequency tunability at this wavelength becomes another important capability. The source frequency can be finely tuned to a nearby gas absorption line for stray light rejection [26,27]. It may also be possible to filter out narrow band non-thermal scattered signals when measuring ion temperature. The problems of stray source light and non-thermal interference with thermal scattering are more severe at MM/FIR wavelengths than at shorter wavelengths. Gas absorption cells can provide many orders of magnitude more narrow band rejection than conventional optical

filters. Also a good narrow band rejection filter may reduce the requirements for beam and viewing dumps and allow for more flexible scattering geometries on constrained access plasma machines.

These advanced MM/FIR source capabilities make possible new design considerations for collective Thomson scattering plasma diagnostics. In this paper we will analyze the trade-offs between source peak-power, output energy, duty factor, and wavelength for optimizing the scattered signal to noise ratio. We will emphasize thermal scattering for ion temperature measurements with brief comparisons to non-thermal scattering requirements. The outline of this paper is as follows: in Section II the performance capabilities of molecular lasers and gyrotrons are presented; in Section III we review collective Thomson scattering theory; in Section IV we present the signal to noise ratio in terms of source peak power, output energy, and duty factor and discuss the limiting cases; in Section V we discuss the application of the advanced source capabilities to optimizing collective Thomson scattering plasma diagnostics and give some examples; and finally in Section VI we present the major conclusions.

## Performance Capabilities of Molecular Lasers and Gyrotrons

Figure 1 shows the estimated power vs. frequency capabilities of molecular lasers and gyrotrons. An output power range is estimated for operation in high peak power pulsed mode, and in high average power/cw mode. The $10\mu m CO_2$ laser power levels shown are those that have been used to optically pump FIR molecular gas lasers. The $CO_2$ laser is a well developed technology which can be operated over a wider range of power levels than shown. The power vs. frequency for the optically pumped molecular lasers and gyrotrons has been estimated as follows:

For optically pumped lasers the power values are estimated for molecular gas lasers excited by $CO_2$ laser pump radiation. The output power $P_o$, at a wavelength $\lambda$, has been roughly approximated assuming

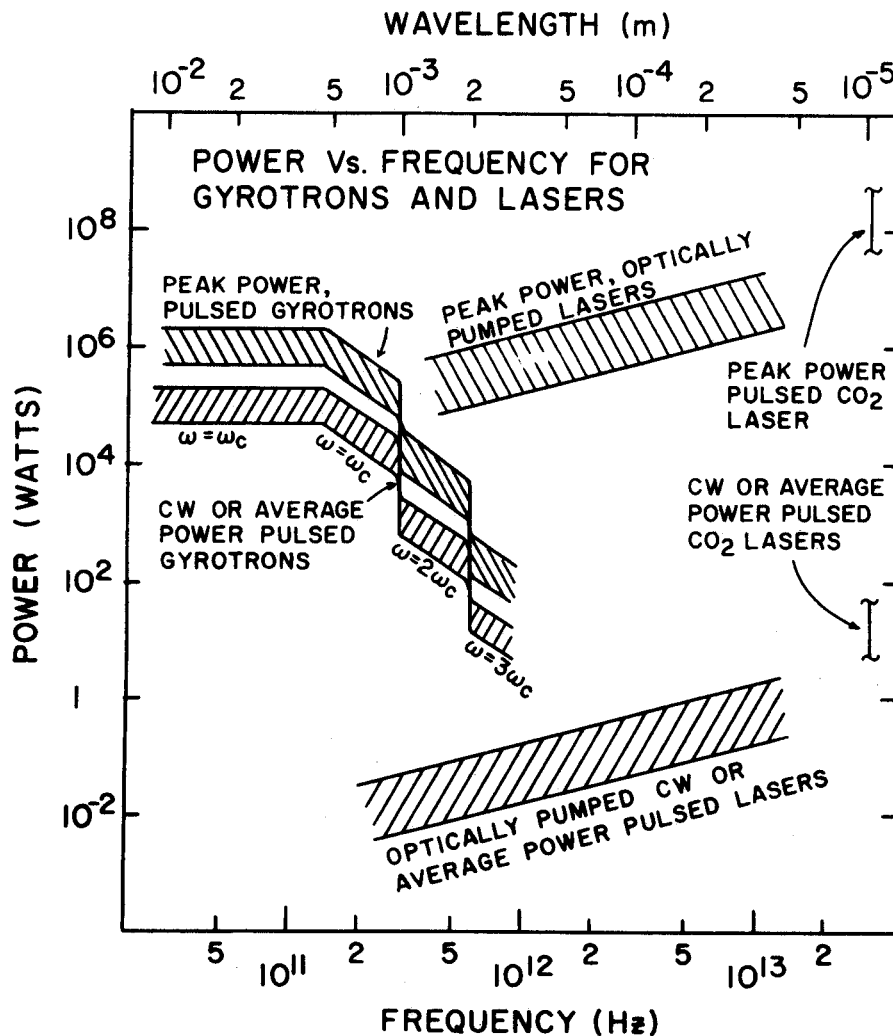$$\frac{P_o}{P_i} \simeq \frac{1}{10} \frac{10\mu m}{\lambda}$$

Figure 1. Estimated power vs. frequency of gyrotrons
and molecular lasers. A power range is
estimated for high peak power pulsed oper-
ation and high average power/cw operation.

where $P_i$ is the incident $CO_2$ laser power, $(10\mu m/\lambda)$ is the
quantum efficiency, and the factor $(1/10)$ is the assumed
efficiency of conversion from $CO_2$ laser photons to far
infrared laser photons. For pulsed lasers, a CO2 pump
pulse of about 500 MW for $10^{-7}$ sec yields an output power
of about 1 MW at $\lambda = 0.5$ mm (600 GHz). In cw operation,
a 50 W, $CO_2$ laser pump yields an estimated output power
of $P_o \simeq 100$ mW. These power estimates are consistent
with experimental results. In repetitively pulsed opera-
tion, the average power of CO2 TEA lasers may be taken to
be about 50 W, a value appropriate over a wide range,
from a 500 J laser which operates at up to 0.1 Hz to a

2.5 J laser at 20 Hz. The peak power of repetitively
pulsed operation is approximately the same as for single
pulse operation.

For gyrotrons, approximate power estimates of cw
operation are based on anticipated gyrotron development
in the United States during the next decade. Cw gyro-
trons operating in the 90 to 140 GHz frequency range,
with 200 kW output power, are scheduled for development
in the U.S. [28]. Very recently 100 kW of pulsed power
(1 µs pulse length) has been obtained at 140 GHz [29].
For frequencies above 140 GHz, gyrotron output power is
assumed to extrapolate as frequency to the (-2.5) power,
based on constant power dissipation per unit area in the
cavity walls. Operation of the gyrotron at the funda-
mental ($\omega = 2\omega_c$) and the estimated output power is re-
duced by a factor of ten because of the lower gain at
that harmonic. For comparison, we note that a 1.5 kW,
cw, 326 GHz gyrotron has been developed by Zaytsev et al.
[30]. This is consistent with a projected power of 2.4
kW, cw at 326 GHz in Fig. 1. At frequencies between 600
and 900 GHz, third harmonic emission is assumed. However,
there is very little experimental data on third harmonic
emission.

Operation of a gyrotron in the short pulse mode
($10^{-7}$ to $10^{-3}$ sec) should allow the gyrotron power to
increase by a factor of about ten over the cw value.
When run in pulsed mode at moderate repetition rate, the
average power of pulsed gyrotrons can possibly approach
that of cw gyrotrons.

The results in Fig. 1 are only intended as rough
estimates, and could be significantly affected by im-
provements in technology and new concepts. Also, a
number of other important sources are available in this
frequency range, such as carcinotrons, EIO's, IMPATT
devices, and ledatrons, although all of these latter
sources have lower average power than the projected values
for gyrotrons. Free electron lasers can provide high
pulsed powers in this frequency range, but at present they
have relatively large bandwidths, unsuitable for scattering
experiments.

## Collective Thomson Scattering Theory

The spectral distribution of Thomson scattered radiation is a function of the parameter

$$\alpha = \frac{1}{k\lambda_D} \simeq \frac{\lambda_o}{4\pi\lambda_D \sin\frac{\theta}{2}} \quad , \tag{1}$$

where k is the magnitude of the difference between the incident and scattered wavevectors, $\lambda_D$ is the Debye length, $\lambda_o$ is the incident wavelength, and $\theta$ is the scattering angle. Collective Thomson scattering refers to scattering from collections or bunches of electrons rather than from individual electrons. This occurs when $\alpha \geq 1$. When this condition is satisfied scattering from electron motions can be correlated with ion motions, plasma turbulence, or plasma waves.

Rearranging Eq. 1, the source wavelength is given by

$$\lambda_o[\text{cm}] = 9.35 \times 10^3 \alpha \sin\frac{\theta}{2} \sqrt{\frac{T_e[\text{eV}]}{n_e[\text{cm}^{-3}]}} \quad , \tag{2}$$

where the minimum usable wavelength for collective Thomson scattering is obtained by setting $\alpha = 1$. It can be readily verified that **MM/FIR** sources are required for collective Thomson scattering in fusion plasmas at angles greater than 1°. Not all wavelengths calculated by Eq. 2 are usable. An upper limit on the maximum $\lambda_o$ or equivalently, a lower limit on frequency, is set by the plasma frequency. Frequencies less than the plasma frequency will not propagate in the plasma. This condition is written as

$$\lambda_o[\text{cm}] < \frac{3.33 \times 10^6}{\sqrt{n_e[\text{cm}^{-3}]}} \cdot \tag{3}$$

A more restrictive upper limit on $\lambda_o$ occurs in the presence of strong magnetic fields

$$\lambda_o[\text{cm}] < \frac{10.7}{\ell B[\text{kG}]} \tag{4}$$

where B is the magnetic field in kG and $\ell$ is the harmonic number of the highest electron cyclotron emission (ECE) harmonic that is optically thick or emits strongly enough to interfere with the scattering measurement. The choice

of $\ell$ in Eq. 4 depends on the details of the plasma experiment including most importantly the electron temperature and the effectiveness of the viewing dump. For most present tokamaks $\ell = 3$, but in future hotter plasmas $\ell$ can be much larger.

The Thomson scattered signal for incident and scattered signal polarization perpendicular to the plane containing the incident and scattered wavevectors is given by

$$P_s = P_o n_e r_e^2 Ld\Omega S(\vec{k},\omega) ,\qquad (5)$$

where $P_s$ is the scattered intensity in $WHz^{-1}$, $P_O$ is the incident power in $W$, $r_e = 2.82 \times 10^{-13}$ cm is the classical electron radius, L is the Length of the scattering volume along the source beam, $d\Omega$ is the solid angle of collection, and $S(k,\omega)$ is the spectral density function [2]. If we assume diffraction limited Gaussian optics $Ld\Omega$ can be approximated as

$$Ld\Omega \simeq \frac{\lambda_o}{F^{\#}\sin\theta} ,\qquad (6)$$

where $F^{\#}$ is the collection optics F - number (ratio of focal length to aperature). For relatively small scattering angles $(0 \leq 10°)$, when an axicon [31] can be used to collect the entire cone of scattered signal at a given scattering angle, $Ld\Omega$ will have its maximum value of

$$Ld\Omega = 2\pi\lambda_o ,\qquad (7)$$

as long as the scattering length in the plasma is smaller than the actual plasma size.

The spectral density function has been analytically derived for the case of thermal scattering from a Maxwellian plasma [1,2]. For our work a useful approximation for $S(k,0)$ can be made which will provide insight into optimizing thermal collective Thomson scattering with respect to wavelength and scattering angle. For simplicity, we assume that the scattering geometry is orientated so that magnetic field effects can be ignored. If we assume $\alpha > 2$, $T_e/T_i = 1$, $Z = 1$ (singly charged ions), then

$$S(\vec{k},0)[Hz^{-1}] \simeq 4.8 \times 10^{-8} \frac{\lambda[cm]}{\sin\frac{\theta}{2}}\sqrt{\frac{m_i[amu]}{T_e[eV]}} ,\qquad (8)$$

where $m_i$ is the ion mass in atomic mass units. A similar dependence on $\lambda_0, \theta, m_i$, and $T_e$ can be shown to exist for other fixed ratios of $T_e/T_i$. In the numerical examples in Section V we used the full equations of [1,2] for the calculations, but Eq. 8 would give the same quantitative results to within 10% and shows how the wavelength and scattering angle can be varied to increase the signal to noise ratio.

Another important parameter for thermal Thomson scattering is the total bandwidth and the required frequency resolution to determine the scattered spectral lineshape. The required frequency resolution (bandwidth of one channel in a receiver) is an important parameter for determining the scattered signal to noise ratio. Generally, this parameter is a compromise between maximum bandwidth for maximum signal to noise ratio and minimum bandwidth for maximum resolution of the scattered spectral lineshape [32]. In this work we will assume that to measure the thermal scattered lineshape we need to measure the half width from frequency center to one fifth intensity of frequency center with eight channels of resolution. Since for $T_e = T_i$ the scattered lineshape does not peak at frequency center, this would be a measurement of the lineshape over a signal intensity range larger than five to one. The bandwidth of one of our frequency channels can be approximated by

$$\Delta f[\text{MHz}] \simeq \frac{3.1 \times 10^{-8}}{\mathcal{S}(\vec{k},0)[\text{Hz}^{-1}]}, \tag{9}$$

where $\mathcal{S}(k,0)$ is given by Eq. 8.

At this point it is useful to compare thermal scattering with non-thermal scattering. There are two major differences; one is in linewidth and the other is in scattered signal strength. The full linewidth of non-thermal scattered features is typically on the order of a few hundred kHz or less [8-13], while the linewidth of the thermal scattered feature in fusion plasmas is on the order of a GHz or more. The difference in scattered signal strengths is best shown by the frequency integrated spectral density functions. For thermal scattering [1]

$$\int \mathcal{S}(\vec{k},\omega)\,d\omega = \mathcal{S}(\vec{k}) \simeq \tfrac{1}{2}, \tag{10}$$

For non-thermal scattering [14]

$$\mathcal{S}(\vec{k}) \simeq n_e V_s \left| \frac{\tilde{n}_e}{n_e} \right|^2 , \qquad (11)$$

where $V_s$ is the scattering volume and $\frac{\tilde{n}_e}{n_e}$ is the fraction of fluctuating electrons. As a numerical example for non-thermal scattering assume a plasma density of $10^{14} cm^{-3}$, a scattering volume of $1 cm^3$ and a fluctuation level of 1%, them $\mathcal{S}(\vec{k}) \simeq 10^{12}$. The signal levels for non-thermal scattering can be many orders of magnitude larger than for thermal. High power sources are not needed to measure high level non-thermal fluctuations as in our example and milliwatt lasers have been successfully used [10], but if much lower non-thermal fluctuations $\left( \frac{\tilde{n}_e}{n_e} \leq 10^{-5} \right)$ are to be measured then high power sources will be needed.

A method to take advantage of the large non-thermal scattering levels to measure ion temperature has been proposed [33]. This method consists of scattering from plasma waves with known dispersion relations which depend on ion temperature. Many of the arguments presented in this paper for optimizing scattered signal levels would apply to this technique as well.

## Signal to Noise Ratio

In this present study we are concerned with optimizing the scattered signal to noise ratio. The resulting accuracy of the ion temperature measurement is a different issue and has been covered in the literature [32,34]. In general, the higher the signal to noise ratio, the lower will be the resulting error in the ion temperature measurement. The signal to noise ratio in one channel is given by

$$S = \frac{P_S}{P_S + P_N} \sqrt{1 + \Delta ft} , \qquad (12)$$

where $P_N$ is the noise power due to the receiver noise and plasma emission, and t is the signal integration time.

In this analysis, we allow source operation to be in any of three different modes, namely cw, repetitively pulsed, or single pulse. All three modes, however, can be treated using the same formalism. Consider a repetitively pulsed source of pulse length $\tau$ and pulse repetition

rate $R_p$. The source is repetitively pulsed N times in a
time interval $t_p$ during which the plasma conditions are
assumed to remain constant. The receiver system is gated
so that scattered radiation is only collected while the
source is pulsed on. Then the total receiver integration
time, t, is given by

$$t = N\tau = R_p t_p \tau = Dt_p \ , \tag{13}$$

where $D = R_p \tau$ is the usual definition of the duty factor.
Both single shot and cw operation correspond to the special
case N = 1 and t = $\tau$. We call this case single shot oper-
ation when the integration time, t = N$\tau$, is small compared
to the characteristic time during which plasma conditions
are constant. When these times are comparable, we refer
to this case as cw operation. If the output power of the
source during a pulse is $P_o$, then the total energy, E,
emitted during the integration time t is

$$E = tP_o \ , \tag{14}$$

while the average power, $P_{av}$, emitted during the measure-
ment time $t_p$ is

$$P_{av} = DP_o \ . \tag{15}$$

Using Equation 14 in Equation 12, we can express the
signal to noise ratio dependence on source energy and
power. There are two limiting cases to Eq. 12 depending
on the strength of the scattered signal. For simplicity,
we assume $\Delta ft \gg 1$.

When the scattered signal level is large relative to
the noise, $P_s \gg P_N$, then

$$S \simeq \sqrt{\frac{\Delta f E}{P_o}} \ . \tag{16}$$

In this limit the signal to noise ratio is limited by the
time-bandwidth product. Eq. 16 shows that reducing the
source peak power while maintaining or increasing the
energy output will increase the signal to noise ratio.
This would be equivalent to increasing the pulse length
in the single shot case or to increasing the duty factor
in the repetitively pulsed case. Effectively, the inte-
gration time would then be longer and the signal to noise

ratio would be improved by the square root increase in integration time.

In the other limit of very small scattered signal levels relative to the noise, $P_S \ll P_N$, Eq. 12 reduces to

$$S \simeq A \sqrt{\Delta f P_O E} \quad , \qquad (17)$$

where

$$A = \frac{n_e r_e^2 \, Ld\Omega \, \mathcal{J}(\vec{k},\omega)}{P_N} \quad .$$

In this limit the signal to noise ratio is power and energy limited. Increasing either or both the source peak power and output energy can improve the signal to noise ratio. A way for increasing peak power without changing energy is by reducing the source duty factor so that the same energy is delivered in higher peak power pulses. The signal to noise ratio would increase proportional to the inverse square root of the duty factor. Also, the diagnostic time resolution or plasma measurement time, $t_p$, would remain unchanged though the signal integration time, t, would decrease. Therefore, in this limit, for sources of the same average power, a repetitively pulsed source would have significant advantages over a cw source. For example, this would be a way to increase the sensitivity of Thomson scattering diagnostics to lower levels of fluctuations, particularly in non-thermal scattering where low power cw sources are presently used.

Other guide lines for increasing the thermal scattered signal to noise ratio can be derived by observing the dependence of Eq. 17 on the coefficient A. Through coefficient A the signal to noise ratio is proportional to $\lambda_o^2$ and $\theta^{-2}$. This can be verified by observing the dependence of $Ld\Omega$ and $\mathcal{J}(k,0)$ on wavelength and scattering angle as given by Eqs. 6 and 8. As a consequence the longest source wavelength up to the limits given by Eq. 3 and 4 and the smallest scattering angle consistent with the required spatial resolution will maximize the signal to noise ratio. The physical interpretation of why this is so can be easily understood. As $\lambda_o$ is increased and $\theta$ decreased the scattered spectral linewidth decreases causing the signal per Hz to increase, also the diffraction

limited scattering volume increases and the signal increases due to a larger scattering volume. Actually, if we take into account the dependence of $\Delta f$ on $\lambda_o$ and $\theta$ as defined by Eqs. 9 and 8, then the signal to noise ratio will be proportional only to $\lambda^{3/2}$ and $\theta^{-3/2}$.

Maximizing the source wavelength and minimizing the scattering angle is equivalent to maximizing the parameter $\alpha$. Scattering at too large an $\alpha$(small $\vec{k}$) will increase the likelihood that the scattering will be from non-thermal fluctuations [8-12]. We feel this may not be a problem for thermal scattering ion temperature diagnostics because of the vast difference in linewidth between thermal and non-thermal scattering. Measurements over several orders of magnitude of signal level show that the non-thermal frequency spectrum falls off either exponentially [12] or by a large inverse power of frequency [10]. If the non-thermal scattered linewidth is on the order of 100 kHz at half maximum and the frequency spectrum falls off exponentially, then the intensity of the non-thermal feature will be negligible at frequency offsets (>100 MHz) typical of thermal scattering. All that is needed is a narrow band rejection filter between the plasma and receiver. Such a filter would probably be required anyway to reject stray source light. The capability of fine tunability of advanced MM/FIR sources becomes important in this case. The source can be tuned to a nearby gas absorption line and the path length through the gas can be made as long as necessary to reject the non-thermal scattered feature while passing the thermal feature [26, 27]. However, there is still little data on low level non-thermal fluctuations at large frequency offsets.


## Discussion and Examples

When designing a collective thermal Thomson scattering diagnostic to measure ion temperature, one must first decide how much of the scattered frequency spectrum must be measured to determine the ion temperature. Secondly, the number of frequency channels needed to resolve the frequency spectrum must be decided. For the purpose of discussion here, as we have stated earlier, we will assume that only the frequency spectrum half width from linecenter to one-fifth intensity of linecenter needs to be measured with eight channels of resolution. The signal to noise

ratio of the Thomson scattering diagnostic is then specified
by the channel with the weakest signal, in our case by
the eighth channel from linecenter. The other channels
will have a signal to noise ratio that is equal or greater.

Using Eqs. 12 and 14 we can plot contours of constant
signal to noise ratio in two dimensional space with axes
corresponding to source output energy and peak power.
Such plots can be used as an aid to visualize the relation-
ship between source performance characteristics and signal
to noise ratio. In Fig. 2a through c, we show such con-
tours for three different source wavelengths correspond-
ing to three different high power source technologies
that are currently available. These technologies are:
the optically pumped 385 $\mu$m $D_2O$ laser, a 140 GHz gyrotron,
and the 10 $\mu$m $CO_2$ laser. The hydrogen plasma temperature
and density are the same for all three plots, $T_e = T_i = 1$keV
and $n_e = 5 \times 10^{13}$cm$^{-3}$. A scattering angle of $30°$ and a
collection optics $F^{\#}$ of 10 were assumed for the $D_2O$ laser
and gyrotron, while for the $CO_2$ laser a scattering angle
of $1°$ and the use of an axicon was assumed. The background
noise was chosen to be equal to $3 \times 10^{-19}$WHz$^{-1}$ which is
the currently demonstrated noise level for submillimeter
wave and $CO_2$ laser heterodyne receiver technologies. A
somewhat lower noise figure is available at 140 GHz, but
for purposes of comparison we will assume the same noise
figure at all three wavelengths. The effect of varying
the noise will be considered later.

The signal to noise ratio contours are a series of
parabolas with the energy minimum occurring for $P_S = P_N$.
At low peak power these contours correspond to the con-
dition $P_S < P_N$ and the limiting case of Eq. 17 would apply
($EP_O$ = const. for S = const.). On the high peak power
side, $P_S > P_N$ and the signal to noise ratio is time-band-
width limited as given by Eq. 16 ($E/P_O$ = const.). It is
clearly evident that achieving high signal to noise ratios
requires not only optimum power, but sufficient energy.
This is why cw or quasi-cw source capability is an impor-
tant advantage. By specifying the source peak power and
energy, the signal integration time is uniquely specified.
In Fig. 2, contours of constant integration time are
shown as dashed diagonals. The actual plasma measurement
time is equal to, or longer than, the signal integration
time depending on the duty factor as $t_p = t/D$.
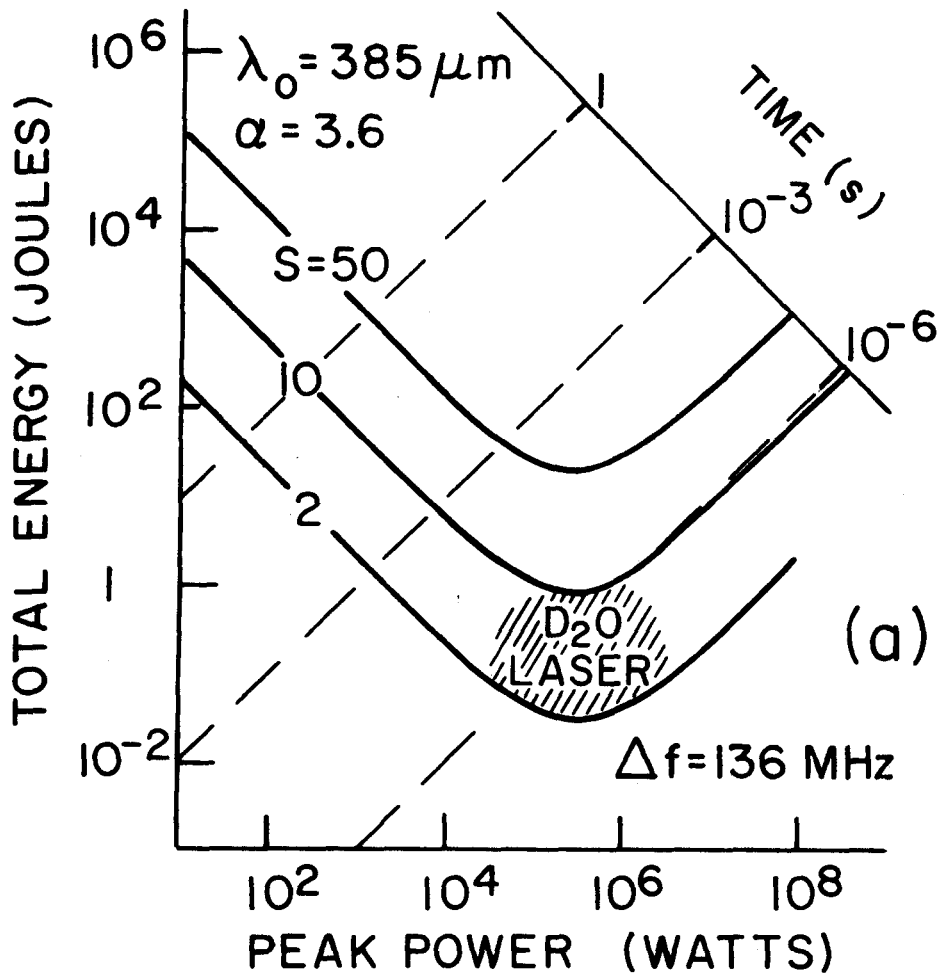
Figure 2a.    Source output energy versus peak power for
              constant signal to noise ratios of 2, 10,
              and 50, for thermal Thomson scattering
              from a hydrogen plasma with $T_e = T_i = 1KeV$
              and $n_e = 5 \times 10^{13} cm^{-3}$.   $P_N$ is assumed to
              be $3 \times 10^{-19} WHz^{-1}$.  Shaded region shows
              approximate operating range for a 385 μm
              $D_2O$ laser source, $\theta = 30°$ and $F^\# = 10$.

The present operating capabilities of $D_2O$ lasers is
superimposed over the signal to noise ratio contours in
Fig. 2a.  These lasers have peak output power capability
between 0.1 and 1MW which is optimum for the plasma con-
ditions used in this example.  Because of limited output
energy these sources are limited to signal to noise ratios
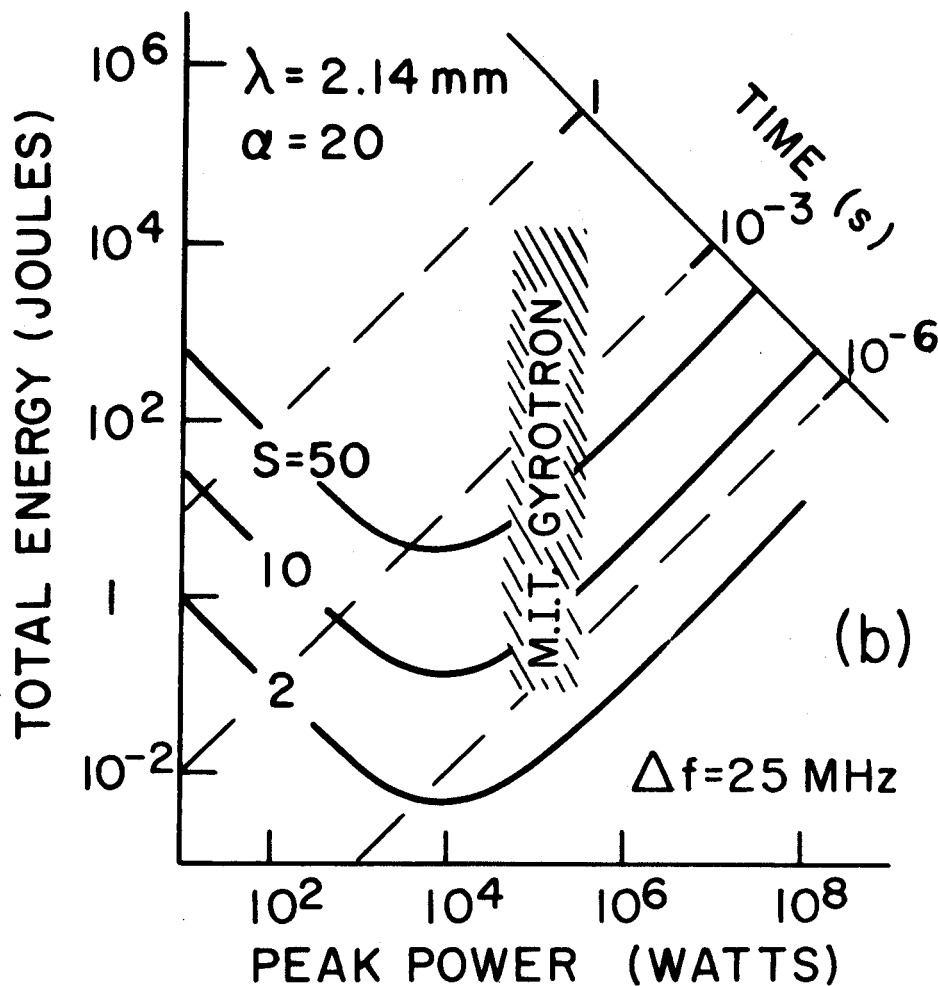of less than 10 for the example chosen.

Figure 2b.    Same plasma conditions as in Fig. 2a.
Shaded region shows approximate operating
range of a 140 GHz gyrotron, $\theta = 30°$, and
$F^{\#} = 10$.

The signal to noise ratio for a pulsed, 140 GHz gyro-
tron is shown in Fig. 2b.  A gyrotron operating at this
frequency has recently been demonstrated at M.I.T. in short
pulse operation (1μs with 100 kW output power [29]).  In
Fig. 2b, it is assumed that the M.I.T. gyrotron can be
extended to long pulse operation, which, based on present
results, appears likely.  First note that at this longer
source wavelength, all signal to noise ratio contour
minima have shifted to lower energies and peak powers so
that 5 to 20kW peak power is optimum.  This is because of
the $\lambda_o^{3/2}$ dependence of signal to noise ratio in the limit
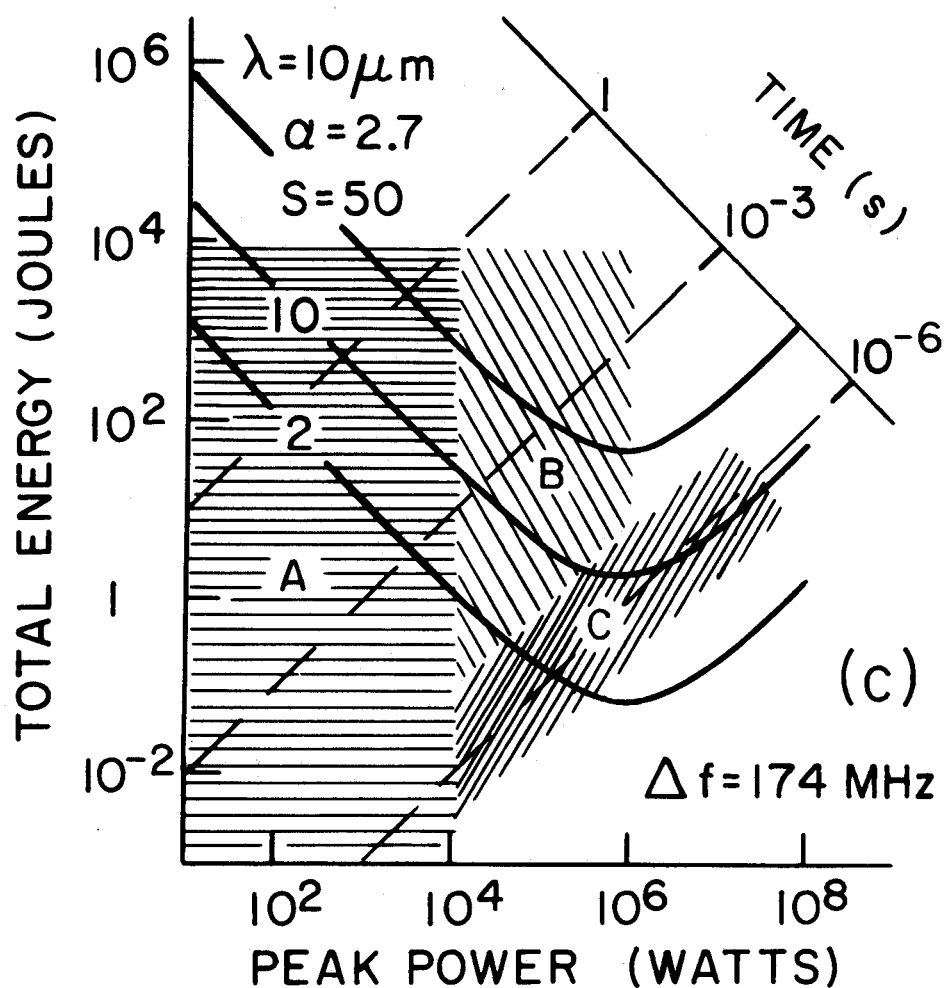$P_s \leq P_N$, as described in Section IV.  The gyrotron output

Figure 2c.　Same plasma conditions as in Fig.2a, but
　　　　　　 using a 10μm $CO_2$ laser and θ = 1° axicon.
　　　　　　 The different shaded regions correspond to:
　　　　　　 A cw operation, B repetitively pulsed, and
　　　　　　 C high power single pulse operation. Lines
　　　　　　 of constant integration time are shown by
　　　　　　 the dashed diagonals and Δf is given by Eq.9.

power of approximately 100kW is more than adequate for
these plasma conditions. Also, because of the high
average power operational capability of gyrotrons, signal
to noise ratios in excess of 50 are possible. The long
gyrotron wavelength of the present example exceeds the
limit for electron cyclotron emission background noise
given in Eq. 4 for magnetic fields greater than 16kG.
Therefore, this particular gyrotron can not be used for
scattering in high field tokamaks. It might be ideal for

present and future low field plasma devices, such as mirror machines. A 94 GHz gyrotron scattering experiment has been proposed for EBT [35]. Higher frequency gyrotrons could be developed as shown in Fig. 1 and thereby increase the limiting magnetic field at which this technology can be used.

The $CO_2$ laser technology is the best developed as shown in Fig. 2c. The scattering angle must be kept relatively small with a wavelength of 10µm to keep $\alpha > 1$. As a result the effect on the signal to noise ratio contours of a short scattering wavelength is largely offset by the small angle. The optimum peak power is therefore about 1 MW, similar to the $D_2O$ laser case. Spatial resolution is largely sacrificed with $CO_2$ laser scattering, but because of the high output energies possible the signal to noise ratio could be very high as in the gyrotron case. Also, the short $CO_2$ laser wavelength is far from the limitations imposed by Eq. 3 and 4 and scattering in most high field, high temperature machines would be possible.

Additional advantages for $CO_2$ laser scattering have resulted from recent technological advances. One such advance is the single-mode fine frequency tunability of high-power $CO_2$ lasers [19,20]. This allows the use of gas absorption cells for stray light control. Another advance is the electrooptically tunable cw $CO_2$ laser with an instantaneously tunable bandwidth which could be as large as 40 GHz [36]. This advance can be used to overcome the bandwidth limitation of $CO_2$ laser mixers.

The development of high power $CO_2$ laser pumped lasers in the wavelength range between the 385 µm $D_2O$ laser and 10µm $CO_2$ laser could provide advantages that combine those of $D_2O$ and $CO_2$ laser scattering. Shorter wavelength optically pumped lasers would be capable of higher power and output energy as shown in Section II by the wavelength scaling of conversion efficiency. Also, shorter wavelength optically pumped lasers would be further displaced in frequency from the ECE background and would have improved diffraction limit focusing. The latter capabilities would be very important for large, high temperature plasmas. At the same time scattering angles greater than with the $CO_2$ laser would be possible for spatial resolution.

THERMAL THOMSON SCATTERING SIGNAL TO
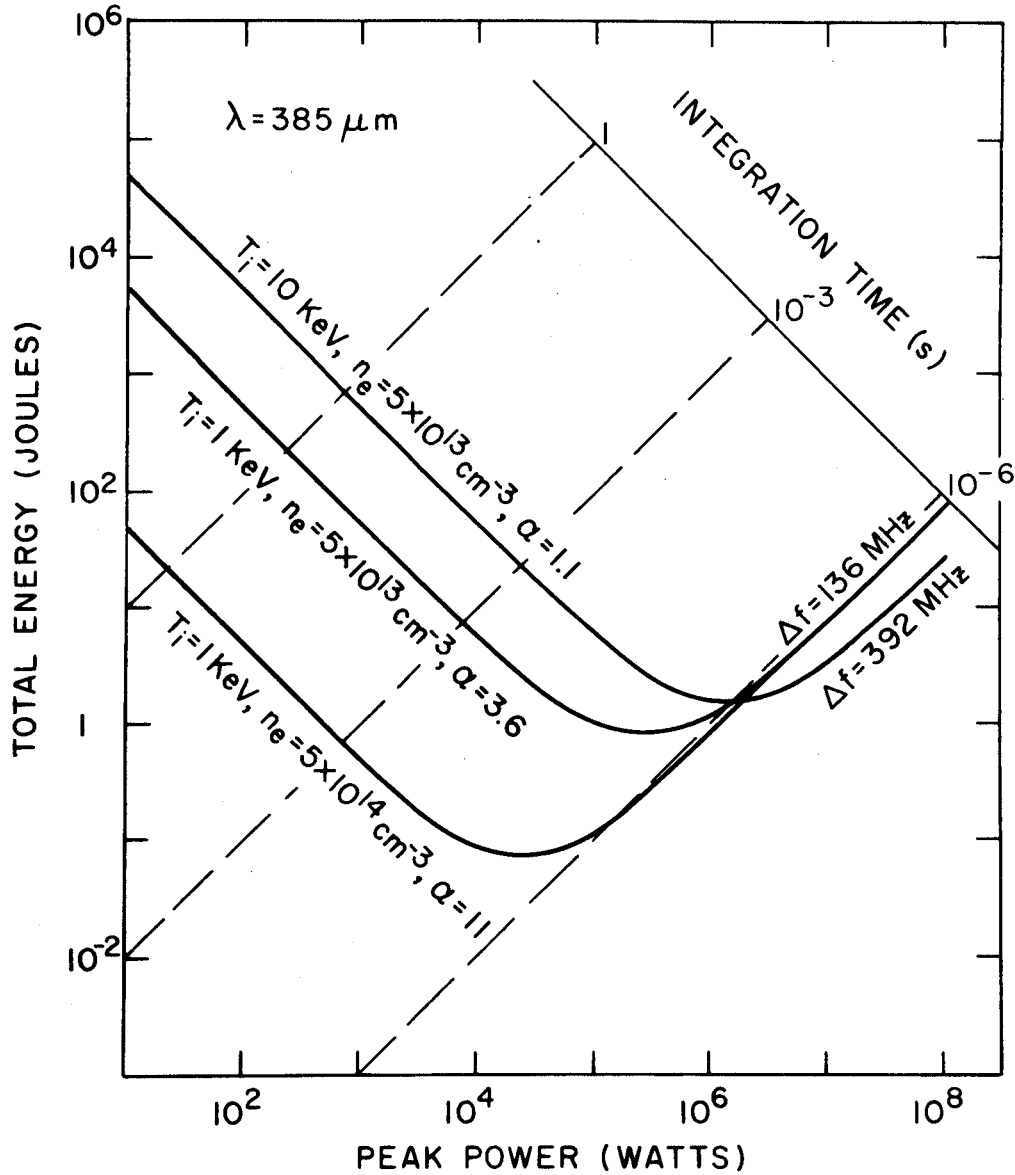NOISE RATIO CONTOURS OF IO FOR VARIOUS
PLASMA PARAMETERS



Figure 3.  Effect of varying the plasma density
from $5 \times 10^{13}$ to $5 \times 10^{14} cm^{-3}$ and the
ion temperature from 1KeV to 10KeV on
the signal to noise ratio of 10 con-
tour for 385µm thermal Thomson scatter-
ing.  All other parameters are the same
as in Fig. 2a.

In Fig. 3 we show the effect of the plasma density and ion temperature on the source requirements for a signal to noise ratio of 10. All other parameters are the same as in Fig. 2a for the 385μm $D_2O$ laser case. Changing the plasma density causes a proportional change, in the limit $P_S \leq P_N$, for both source peak power and energy requirements. At high plasma densities source performance requirements can be significantly reduced. Changing the ion temperature, on the other hand, requires only a change in required source peak power approximately proportional to $\sqrt{T_i}$ (when $\alpha > 2$), to keep the signal to noise ratio constant. In the specific example of Fig. 3, the source peak power requirements in the limit $P_S \leq P_N$, changed proportional to $T_i$ because $\alpha < 2$ at $T_i = 10KeV$. The required source energy at optimum power level is approximately independent of ion temperature. This is because the scattered signal bandwidth varies with ion temperature and the resolution bandwidth can be adjusted to keep the requirements on source energy constant.

The effect of varying background noise on the signal to noise ratio is shown in Fig. 4. In this figure the plasma scattering conditions are the same as Figs. 2a and b except the source wavelength is assumed to be 1mm. All the contours correspond to a signal to noise ratio of 10. High noise powers require proportionally higher peak power and output energy sources when $P_S \leq P_N$. It may be possible to overcome plasma ECE emission in some cases by developing high enough peak power and output energy sources. On the other hand, in quiet plasmas the receiver noise will set a lower limit on the required source performance. For example, this would be an advantage at the 140 GHz gyrotron frequency where lower noise receivers are available.

A comparison of non-thermal scattering with thermal scattering is made in Fig. 5. Again, we plot contours of signal to noise ratio equal to 10 for source wavelength 1mm, and the same plasma conditions as in Fig. 2a and b. The non-thermal fluctuations are assumed to have a bandwidth of 1MHz and a scattering volume of 1cm$^3$. The most noticeable difference of the non-thermal signal to noise ratio contours is the shift to lower peak power levels and longer integration times due to the narrower bandwidth. As the fraction of non-thermal fluctuations increases the required source performance for both output
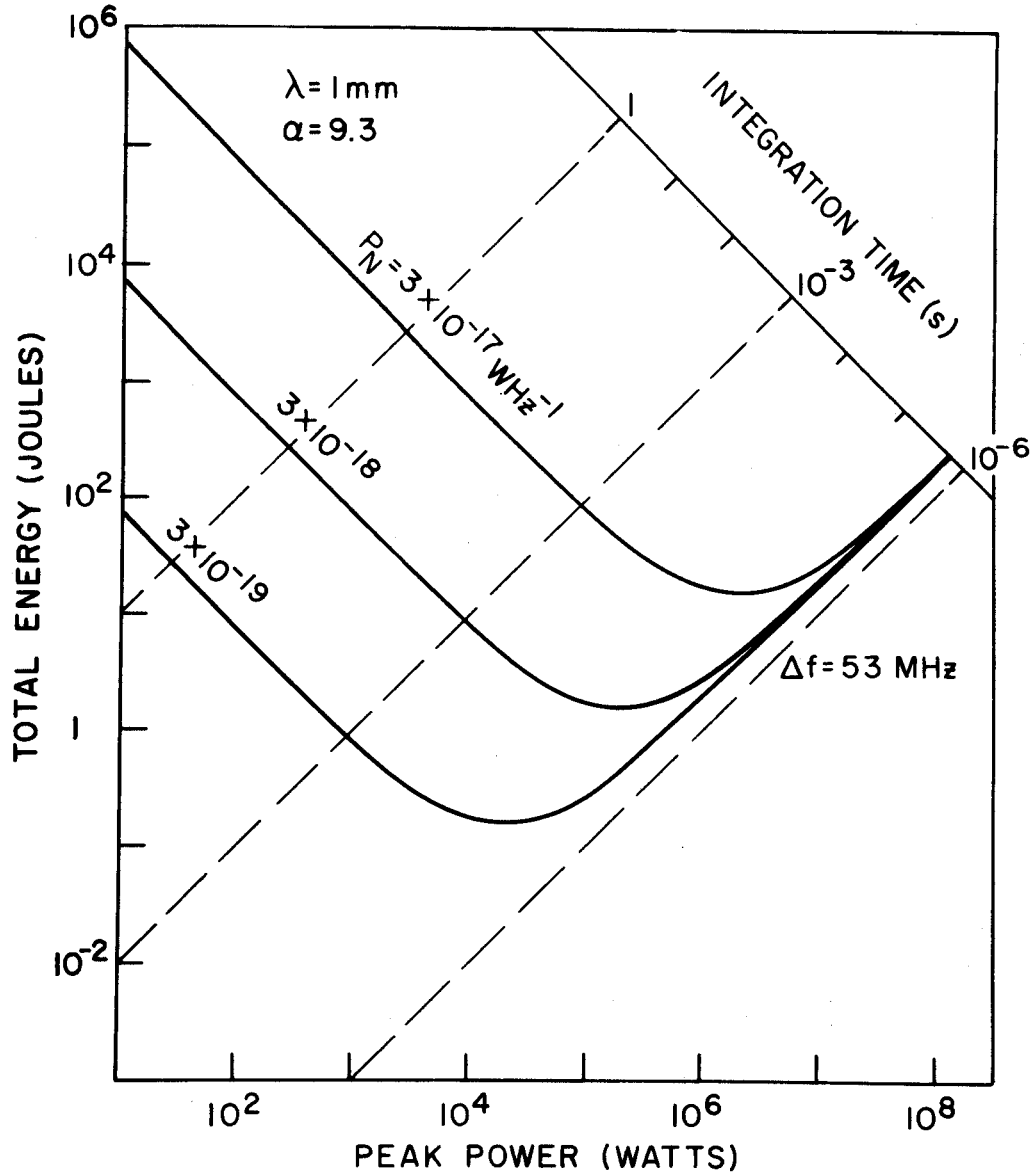
Figure 4. Effect of varying noise power on
thermal Thomson scattering signal
to noise ratio of 10 contour.
Assumed conditions: $H_2$ plasma,
$T_e = T_i = 1KeV$, $n_e = 5 \times 10^{13} cm^{-3}$,
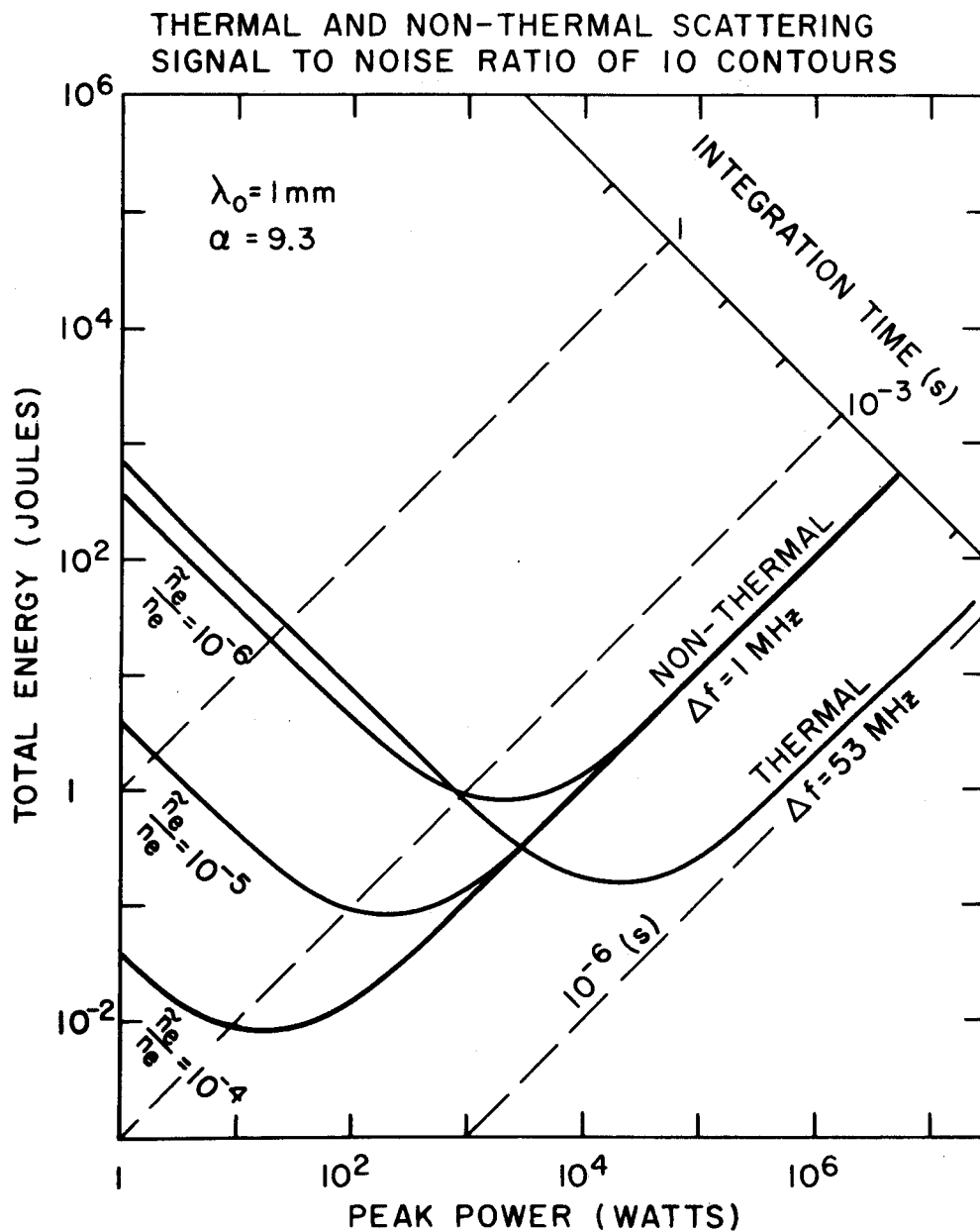$\lambda_o = 1mm$, $\theta = 30°$, $F^\# = 10$.

Figure 5.   Comparison of thermal with low level non-
thermal Thomson scattering.  Signal to
noise ratio of 10 contours plotted for
$H_2$ plasma, $T_2 = T_i = 1KeV$, $n_e = 5 \times 10^{13}$
$cm^{-3}$, $\lambda_0 = 1mm$, $\theta = 30°$, $F^{\#} = 10$, $P_N = 3 \times 10^{-19} WHz^{-1}$.  For non-thermal fluctu-
ations, $V_s = 1cm^3$ and $\Delta f = 1MHz$ assumed.

energy and peak power decreases proportionately.  Milli-
watt level cw FIR lasers have been used to scatter from
non-thermal fluctuations of 0.1 to 1%.  Rapidly pulsing
these lasers and gyrotrons in the 10-100W range can
greatly extend the sensitivity of this technique to fluc-
tuation levels orders of magnitude smaller.


## Conclusions

We have studied how collective Thomson scattering
signal to noise ratio can be optimized by taking advan-
tage of advances in the technology of high power MM/FIR
sources.  These advanced source capabilities include:
cw and quasi-cw operation, flexibility in choice of
wavelength, and fine frequency tunability.  Optimizing
the peak power alone is not enough to assure high signal
to noise ratios.  Adequate output energy is also required.
Source technologies such as the gyrotron and $CO_2$ laser
can provide both high energy and high power.  Present
optically pumped FIR lasers are relatively energy poor,
however, they operate in an important range of wavelengths
intermediate to the gyrotron and $CO_2$ laser.  This wave-
length range is attractive because these wavelengths are
long enough for large angle spatially resolved scattering,
but short enough to avoid severe limitations due to plasma
emission.  Optically pumped lasers with wavelengths shorter
than the 385μm $D_2O$ laser should have improved output
energy capabilities because of a more favorable conversion
efficiency of pump photons.

In cases where the source output energy is sufficient-
ly high but the peak power is less than optimum, increased
peak power through rapid pulsing could be used to increase
the signal to noise ratio.  Conversely, where output energy
is low but peak power is higher than optimum, e.g. single
pulse sources, rapidly pulsing at lower peak power to in-
crease the output energy would increase the signal to
noise ratio.  Rapidly pulsed systems also make possible
time dependent thermal scattering measurements with high
power sources which can only be operated in the pulsed
mode.

Fine frequency tunability of high power MM/FIR sources
combined with narrow-band, gas absorption cells is another
important capability for stray source light rejection.

Also, it may be possible to use such a filter for rejection of narrow band non-thermal scattering when thermal scattering to measure ion temperature. We have shown that large $\alpha$ scattering with the largest scattering wavelength consistent with the plasma frequency and ECE background limits, and the smallest scattering angle consistent with the desired spatial resolution, will maximize the signal to noise ratio.

## Acknowledgements

## References

1. M.N. Rosenbluth, N. Rostoker, Phys. Fluids 5 (1962) 776.

2. J. Sheffield, Plasma Scattering of Electromagnetic Radiation, Academic Press, New York (1975).

3. W.A. Peebles, W.J. Herbst, IEEE Trans. Plasma Sci. PS-6 (1978) 564.

4. D.L. Jassby, D.R. Cohn, B. Lax, and W. Halverson, Nucl. Fusion 14 (1974) 745.

5. H.C. Praddaude and P. Woskoboinikow, NASA Contractor Report 2794 (1978).

6. D.E. Evans, M.L. Yeoman, Phys. Rev. Lett. 33 (1974) 76.

7. W. Kasparek, K. Hirsch, E. Holzhauer, Plasma Phys. 22 (1980) 555.

8. R.E. Slusher, C.M. Surko, Phys. Rev. Lett. 40 (1978) 400, 593.

9. E. Mazzucato, Phys. Fluids 21 (1978) 1063.

10. A. Semet, A. Mase, W.A. Peebles, N.C. Luhmann, S. Zweben, Phys. Rev. Lett. 45 (1980) 445.

11.   C.M. Surko, R.E. Slusher, Phys. Fluids 23 (1980) 2425.

12.   T. Saito, Y. Hamada, T. Yamashita, M. Ikeda,
      M. Nakamura, S. Tanaka, Nucl. Fusion 21 (1981) 1005.

13.   F.F.M. Pots, J.J.H. Coumans, D.C. Schram, Phys.
      Fluids 24 (1981) 517.

14.   T. Tsukishima, in Diagnostics for Fusion Experiments,
      ed. by E. Sindoni, C. Wharton, Pergamon Press,
      Oxford (1979) 255.

15.   C.M. Surko, R.E. Slusher, D.R. Moler, M. Porkolab,
      Phys. Rev. Lett. 29 (1972) 81

16.   D.R. Baker, Meyer Heckenberg, J. Meyer, IEEE Trans.
      Plasma Sci., PS-5 (1977) 27.

17.   C.M. Surko, R.E. Slusher, J.J. Schuss, R.R. Parker,
      I.H. Hutchinson, D. Overskei, L.S. Scaturro, Phys.
      Rev. Lett. 43 (1979) 1016.

18.   G. Ichtcenko, M. Moresco, A. Vendramin, E. Zilli,
      Intl. J. Infrared and Millm. Waves 2 (1981) 713.

19.   P. Woskoboinikow, H.C. Praddaude, W.J. Mulligan,
      D.R. Cohn, B. Lax, Appl. Phys. 50 (1979) 1125.

20.   T. Okada, K. Kato, R. Noudomi, K. Muraoka, M. Akazaki,
      Sixth Intl. Conf. on Infrared and Millimeter Waves,
      Conf. Digest IEEE Cat. No. 81 CH1645-1, MIT (1981)
      M-3-4.

21.   V.A. Flyagin, A.V. Gaponov, M.I. Petelin, V.K.
      Yulpatov, IEEE Trans. MTT-25 (1977) 514.

22.   M. Murphy, G. Haas, 9th Symposium on Engineering
      Problems of Fusion Research, IEEE Pub. No. 81
      CH1717-2 NPS (1981) 2101.

23.   K.E. Kreischer, R.J. Temkin, in Infrared and Millimeter
      Waves, Vol 7, K.J. Button, editor, Academic Press,
      N.Y. (to be published).

24.   D.G. Biron, B.G. Danly, R.J. Temkin, B. Lax, IEEE
      J. Quant. Elec., QE-17 (1981) 2146.

25. P. Mathieu, J.R. Izatt, Optics Lett. <u>6</u> (1981) 369.

26. P. Woskoboinikow, W.J. Mulligan, D.R. Cohn, R.J. Temkin, H.R. Fetterman, 1982 IEEE Intl. Conf. on Plasma Science, Carleton University, Ottawa, Canada, Conf. Record IEEE Cat. No. 82CH1770-7.

27. R.J. Temkin, in Summary of USA-Japan Workshop on Sub-Millimeter Diagnostic Technique, Institute of Plasma Physics, Nagoya University, Nagoya, Japan (1982).

28. U.S. Department of Energy, "Development and Technology Programs to address Research and Development Needs of the Engineering Test Facility," U.S.D.O.E. Report DOE/ER-0073, October, 1980.

29. R.J. Temkin, K.E. Kreischer, W.J. Mulligan, S. MacCabe and H.R. Fetterman, "A 100 kW, 140 GHz Pulsed Gyrotron," in International Journal of of Infrared and Millimeter Waves, 3 (1982) 427.

30. N.I. Zaytsev, T.B. Pankratova, M.I. Petelin, V.A. Flyagin, Radio Eng. Electron Phys. <u>19</u> (1974) 103.

31. J.K. McLeod, J. Optical Soc. Amer. <u>44</u> (1954) 592.

32. L.E. Sharp, A.D. Sanderson, D.E. Evans, Plasma Phys. <u>23</u> (1981) 357.

33. P. Lee, N.C. Luhmann Jr., H. Park, W.A. Peebles, R.J. Taylor, Ying Xu, C.X. Yu, in Summary of USA-Japan Workshop on Sub-Millimeter Diagnostic Techniques, Institute of Plasma Physics, Nagoya University, Nagoya, Japan (1982).

34. M.A. Dupertuis, "Mesure De $T_i$ Et De $Z_{eff}$ Par Diffusion Thomson Dans un Tokamak," LRP 185/81, CRPP, Ecole Polytechnique Federale de Lausanne-Suisse (1981).

35. L. Bichel, T.L. White, Collective Scattering of Gyrotron Radiation for $T_i$ Measurements on EBT, ORNL/TM-7574, Oak Ridge National Laboratory (1981).

36. G. Magerl, P.W. Froehling, IEEE Trans. <u>MTT-30</u> (1982) 220.